IOP Conf. Series: Materials Science and Engineering **202** (2017) 012040 doi:10.1088/1757-899X/202/1/012040

Study of Raman Spectra of Aluminum Powder-Substituted Barium Hexaferrite (BaM) $BaFe_{12-x}Al_xO_{19}$ as a Result of Solid State Reaction Process

S Mustofa[1], R Rizaldy[2] and W A Adi[1]

[1]Center for Science and Technology of Advanced Materials (PSTBM), National Nuclear Energy Agency of Indonesia (BATAN), Kawasan PUSPIPTEK Serpong, Tangerang Selatan, Banten, Indonesia 15314
[2]Dept. of Physics, Faculty of Science and Technology, UIN Syarief Hidayatullah Jakarta, Jl. Ir. H. Juanda No. 95 Ciputat, Tangerang Selatan, Banten, Indonesia 15412

Email: s_mustofa@batan.go.id

Abstract. Aluminum-substituted barium hexaferrite (BaM) that have the general formula of $BaFe_{12-x}Al_xO_{19}$ (x: 0, 1, 2, 3, 4, and 5) was obtained through the process of solid state reaction. The samples of Aluminum-substituted barium hexaferrite (BaM) were characterized using XRD to determine the phase structure, and by Raman Spectroscopy to know the chemical composition and structure. The single phase was obtained for the samples x = 0 - 4 from the weight percentage of the phase, and the other phase i.e. Al_2O_3 and BaO have been achieved for the sample x = 5. The characterization of Raman spectrum on Aluminum-substituted barium hexaferrite (BaM) has been carried out using Bruker SENTERRA instrument. The presence of sharp peaks corresponded to A_{1g} mode shows the possibility of Al substitution in the barium hexaferrite system without any distortion in crystal symmetry. It is also observed that the substitution of A_l in the $BaFe_{12}O_{19}$ system leads to an increase in the intensity of resonance band when compared with the parent compound, which indicates a large polarizability variation during the vibrations in the Aluminum-substituted $BaFe_{12-x}Al_xO_{19}$ compounds.

Keywords : Raman, Al, BaM, $BaFe_{12-x}Al_xO_{19}$, polarizability

1. Introduction

Since the discovery in 1930, hexagonal ferrite or hexaferrite is very interesting for developed.. Hexaferrite materials are materials that are crucial both commercially and technologically, which is marked by the global fabrication of magnetic material for many kinds of applications and uses of these materials. Barium hexaferrite is often applied as a permanent magnet for the applicationsof magnetic recording material (recorder), data storage (hard drive), and a component in electronic devices (sensor), as well as an electromagnetic wave absorbing material [1].

Hexagonal ferrites family are aunique materials that divided into six types, namely M-type ($BaFe_{12}O_{19}$ or $SrFe_{12}O_{19}$), Z-type ($Ba_3Me_2Fe_{24}O_{41}$), Y-type ($Ba_2Me_2Fe_{12}O_{22}$), W-type ($BaMe_2Fe_{16}O_{27}$), X-type ($Ba_2Me_2Fe_{28}O_{46}$), and U-type ($Ba_4Me_2Fe_{36}O_{60}$), where Me can be inserted with the elements of Sr, Co, Ni, or Zn. All hexaferrite families have ferromagnetic properties. Principally, the magnetic properties of hexaferrite family are associated with the crystal structure because hexaferrite has Magnetocrystalline Anisotropy (MCA), which means the magnetization has a tendency towards the

orientation in the crystal structure [2]. One of the ferrite families that attract interest from many researchers in the last few decades is the family of M-type hexaferrite ($BaFe_{12}O_{19}$), which has the empirical equation of BaO.6 (Fe_2O_3). This compound is very cheap and easy to be produced because of its more simple chemical formula than those of other materials in hexaferrite family. The bafe12o$_{19}$ compound has a high electrical resistivity of about 108 Ω cm, a high uniaxial magnetic anisotropy along the c axis, and a high magnetic saturation value that can potentially be applied as a permanent magnet [3-4]. In crystallography, $BaFe_{12}O_{19}$ has a hexagonal crystal structure, with a space group of P 63/mmc (194) and lattice parameters of $a = b = 5.9291$ Å and $c = 23.4070$ Å [5].

In the progress of research developments, the $BaFe_{12}O_{19}$ compound is often modified in such a way for further purposes and different applications, such as for absorption of electromagnetic waves in a high frequency (GHz scale), as the radar absorption material, whether in the field of health or stealth technology [6]. In such applications, Barium Hexaferrite is often substituted with other ions. Several studies have been focused on the ion substitution by Fe^{3+}, which is the only ion that has a magnetic moment, by recombination with other ions that can give an effect to the magnetic properties of the material. Such material is required to have permeability and permittivity with ratios appropriate [7] for the applications as an absorption of the electromagnetic wave. Barium Hexaferrite has a quite high level of permeability and permittivity. Engineering material is needed by substituting the Fe^{3+}magnetic ion with a non-magnetic ion, such as Al^{3+} [8-9] to improve the absorption ability.

In this research, we developed the Al^{3+} ion-substituted barium hexaferrite to obtain the formula of barium hexaferrite that has high permeability and permittivity, and also good absorption ability for the application as an absorbing material for an electromagnetic wave in order to prepare raw materials of anti-radar paint. In accordance with this entire research, this report was based on the analysis of the X-ray diffraction pattern and the crystal structure of the material using the Rietveld method to obtain the accurate crystal structure from the sample, by replicating the crystal structure that already existed in the database so that it complied with the diffraction pattern observation using least squares contained in GSAS-EXPGUI software. Furthermore, an analysis using Raman Spectroscopy to know the chemical composition and structure was also conducted.

1.1. Material of Barium Hexaferrite

The M-type of Hexagonal Ferrite, with the general formula of $BaO.6Fe_2O_3$, has a lattice constant of $a = 5.89$ Å and $c = 23.19$ Å in a hexagonal closed packed of crystal system, which is composed of Oxygen and Barium with Fe in octahedral (12k, 4f2 and 2a), tetrahedral (4f1), and bipyramidal trigonal / hexagonal (2b). Fe cation is a single source of the magnetic moment in this system, which have an upward spin direction in the positions of 12k, 2a, and 2b, and have a downward spin direction [10] in the position of 4f1 and 4f2, as shown in Figure 1. The general structure of the M-type Hexaferrite ($AO.6Fe_2O_3$ or $AFe_{12}O_{19}$, where A is the divalent ions, such as Ba^{2+}, Sr^{2+}, Pb^{2+}, and so on) was hexagonal with a space group of P 63/mmc, consisting of 4 blocks with the symbols of S, S*, R, and R* as shown in Figure 1. Oxygen atoms stacked covered with Ba and Fe atoms in an interstitial place. There are 10 layers of oxygen atoms along with the c axis and Fe atoms located at five different places in crystallography [10].

Among the twelve ions of Fe^{3+} in the formula unit, Fe atom in the position of 4f1 is coordinated tetrahedrally with oxygen, while the Fe atom in the position of 2b was coordinated with five oxygen ions. There is a short distance of Fe-Fe in the structure, and the distance of Fe-Fe Å at the position of 4f2 was ±2.7. Fe ions in the position of 12k of a network with each Fe connected with four ions of another Fe in the same layer [10].

In the form of spin, one ion in the 2b layer on the R block was pointing upwards, and two ions of octahedral led down, and seven octahedral ions on the block S led down. Because each of Fe^{3+} ion contributed $5\mu_B$ at absolute zero of magnetic moment, the total magnetization at zero temperature can be calculated. As known, eight Fe^{3+} ions have an upward spin, and four ions have a downward spin, which resulted in four Fe^{3+} ions with an upward spin. Therefore, the total magnetization per unit molecule is $(1 - 2 + 7 - 2)\ x5\mu_B = 20\mu_B$ [10].

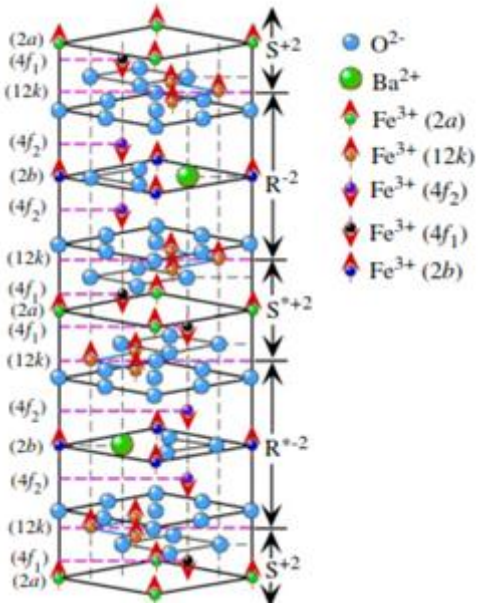

Figure 1. Schematic crystal structure of Barium Hexaferrite [11]

1.2. Aluminum Substituted Barium Hexaferrite

The combination of the intrinsic magnetic properties and electrical properties of such Ferrite are placing a magnetic material of Ferrite as a buffer of electromagnetic waves, especially in micro scale, including the waves with frequencies used in Radar [12]. Nevertheless, the modification by ion substitution is often carried out to increase the non-magnetic permittivity properties so that it can add higher frequency of the power absorption. For example as reported by *Priyono & Azwar* by substituting Ti^{4+} and Mn^{2+} with Fe^{3+} inside the material of Barium Hexaferrite [12]. Evidently, the power absorption of electromagnetic waves could be increased higher than before the substitution. In addition to the substitution of Fe^{3+} ion, substituting Sr^{2+} ion with Ba^{2+} ion was also reported and resulting in a more maximum absorption power [7].

The studies on the substitution of various cations with the crystal structure of Barium Hexaferrite have indicated that it can change the magnetic properties. The focus of this research was the substitution of Al^{3+} ion. According to Dianne & Yokoviev et al. (1969), Al^{3+} ion could substitute Fe^{3+} ion in the system of $BaFe_{12}O_{19}$, depending on the number and positions occupied by Al^{3+} ion, and therefore it could change the magnetic properties [13]. It is well known that Fe^{3+} ion that has a magnetic moment of $5\mu_B$ will be replaced by Al^{3+} ion that has a zero magnetic moment. The magnetic moment of Al^{3+} ion ($0\mu_B$) cannot be removed if it has downward moment direction of spin from the Fe^{3+} ($5\mu_B$). Therefore, the substitution of Al^{3+} ion lead to the weakening superexchange interactions from $Fe_A^{3+} - O - Fe_B^{3+}$, which led to the collapse of magnet collinearity in the crystal lattice structure of Barium Hexaferrite [14].

2. Experimental Method

2.1. Rietveld refinement method

The basis for multiphase profile analysis of powder diffraction patterns was firstly introduced completely by Rietveld in 1969. Rietveld showed the possibility of replicating the results of diffraction

pattern measurements with pattern calculation. The advantage of such pattern calculation is when there is an occurrence of an error that is caused by an intensity deviation in an imperfect model structure, it will tend to leave the remaining intensity, both negative and positive.

The basic principle of Rietveld analysis is to match (fitting) the peak profile of the calculation with the peak profile of the observation. The profile matching (fitting) is carried out by applying the procedure of a nonlinear least square calculation. Expressed as a minimum objective function as follows:

$$S_{Min} = \sum_{i=1}^{N} w_i [y_i(obs) - y_i(cacl)]^2 \quad (1)$$

w_i is weighting factor, i.e. $1/[y_i(obs)]$ that equal FWHM, $y_i(obs)$ is the intensity obtained from observation, and $y_i(calc)$ is the intensity obtained from calculations [15].

The intensity value of profile diffraction pattern at certain positions of Bragg angle can be calculated after correction by entering a function of scale, profile, and background, that is:

$$y_i(calc) = \sum_h s.|F_{hkl}|_h^2.p_h.L(\theta).M_h.pV(\Delta T)_h + y_{ib}(calc) \quad (2)$$

Where $y_i(calc)$ is the intensity taken from calculation, *s* is scale factor, *F* is structure factor, *p* is the multiplicity factor, $L(\theta)$ is Lorentz-polarization factor, M is temperature factor, $pV(\Delta T)$ is geometry factor (function profile: Pseudo-Voigt), $y_{ib}(calc)$ is function of background [16].

2.2. Degrees of Conformity

To determine the success of a smoothing, it needs a standard value which indicates the quality of the smoothing. In GSAS use least square smoothing that is indicated by some residual function, which is set in a particular way in each histogram.

2.3. Software GSAS-EXPGUI

GSAS stands for General Structure Analysis System created by R.B. Von Dreele and A.C. Larson. This program is based on the Rietveld smoothing method. GSAS is a set of programs for processing and analyzing single crystal diffraction data and powder obtained by the characterization of x-ray diffraction. GSAS can handle data of powder diffraction pattern from phase mixture by softening the structure parameters of each phase. The collected data that are ready to be input into the EXPGUI GSAS will be processed through qualitative and quantitative analysis by Rietveld smoothing method.

2.4. Preparation of Powder Materials of $BaAl_xFe_{12-x}O_{19}$ (x: 0 – 5)

The powder materials of $BaAl_xFe_{12-x}O_{19}$ (x: 0 - 5) used for characterization by XRD (SHIMADZU 700 XRD) and Raman Spectroscopy have been prepared through the process of synthesis using basic powder materials of $BaCO_3$, Fe_2O_3, and Al_2O_3. The synthesis process was performed by solid state reaction method using HEM (High Energy Milling) equipment for 7 hours, which consist of 5-hour milling and 2-hour break, and then the powder materials were burnt for 5 hours at a temperature of 1000 ^oC.

2.5. Characterization of Raman Spectra

The samples were characterized using Raman Spectrometer (Bruker SENTERRA) for microstructural analysis. The Raman Spectroscopy system employed in this study consisted of 1 mW – 100 mW lasers with 785 nm wavelength, single grating 0.5 m spectrometer single grating, charged – coupled device (CCD) detector, and holographic optics. A spectrum range of 400 to 1800 cm^{-1} at room temperature was examined in this study using a grating of 1800 grooves/mm. A 60-minute exposure time was used for recording the Raman spectrum.

3. Results and Discussion

3.1. XRD Pattern

Figure 2 shows the XRD pattern of the samples, which is a modification of the Barium Hexaferrite system by the addition of Al element into Fe with variations of x = 0, 1, 2, 3, 4 and 5. The XRD results of Barium Hexaferrite samples showed that the suspected different phase came after the addition of Al into Fe. A further phase identification is required concerning the COD. Phase identification of raw data was carried out by using software of XRD Match! 2 that refer to COD based on the information of peak position and intensity as shown in Figure 2.

From the matching peak using software for further identification, the phase of $BaFe_{12}O_{19}$, $BaAl_{2.18}Fe_{9.82}O_{19}$, Al_2O_3, and BaO were obtained, which respectively refer to the research findings of Obradors et al. [5] at a ground state level (x = 0), Sandiumenge [8] for x = 1 - 5, and Wang et al. [17] and Wyckoff et al. [18] for the additional phase at x = 5.

After the information phases from peak matching using software have been obtained, then a further analysis was carried out to determine the effect of Al substitution on the crystal structure of Barium Hexaferrite. To analyze the pattern of XRD and to find out more information about crystallography from the samples, the Rietveld smoothing method with the help of software GSAS-EXPGUI was needed. Samples x = 0 is the ground state of the system Barium Hexaferrite, without any substitution of Al^{3+} ion. Rietveld refining results are illustrated in the form of the red plot for data calculation and green for observation data, along with the blue curve after subtraction of the background function, as shown in Figure 3.

The results of smoothing have a matching degree that is convergent. Therefore it is believed that there was a single phase of Barium Hexaferrite at x = 0. The crystallographic information and the level of compatibility are shown in Table 1.

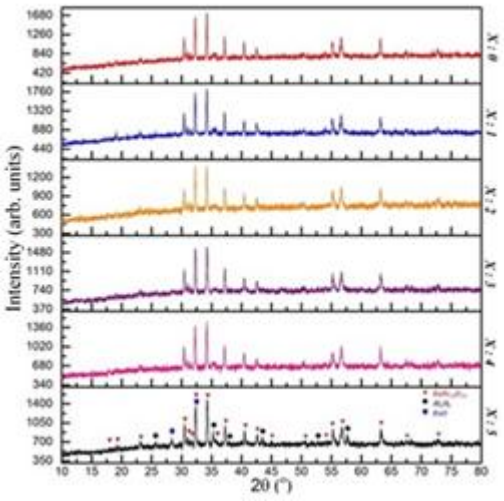

Figure 2. XRD pattern for Barium Hexaferrite $BaFe_{12-x}Al_xO_{19}$ with Al^{3+} ion substitution (x = 0 - 5)

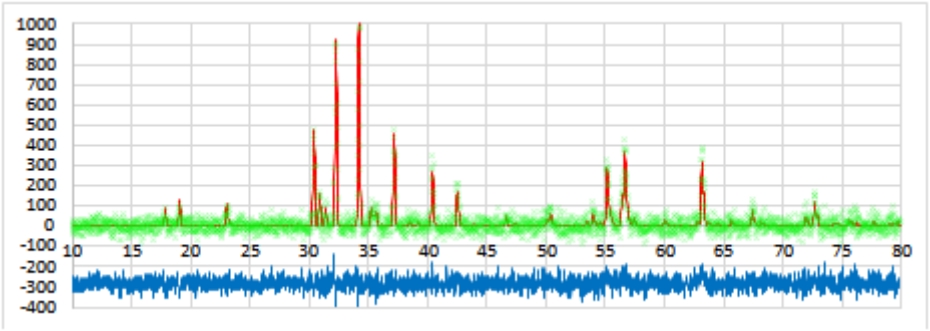

Figure 3. The smoothing results of XRD pattern of $BaAl_xFe_{12-x}O_{19}$ (x = 0)

Table 1. Parameter structure, factor R and x^2 of $BaAl_xFe_{12-x}O_{19}$ (x = 0)

				Lattice Parameters		
Space Group	:	P 63/m m c				
Crystal system	:	Hexagonal		a = 5.886965 Å	b = 5.886965 Å	c = 23.188545 Å
Volume	:	695.964 Å^3				
Article I. (ρ)	Density :	Article II. g.cm^{-3}	5.304	$\alpha = 90^o$	$\beta = 90^o$	$\gamma = 120^o$
Factor R				wRp = 3.86	Rp = 3.06	x^2 = 1.121

Table 2. Parameter structure, factor R and x^2 of $BaAl_xFe_{12-x}O_{19}$ (x = 1)

			Lattice Parameters		
Space Group	:	P 63/m m c			
Crystal system	:	Hexagonal	a = 5.88659 Å	b = 5.88659 Å	c = 23.18459 Å
Volume	:	695.757 Å^3			
Density (ρ)	:	5.136 g.cm^{-3}	$\alpha = 90^o$	$\beta = 90^o$	$\gamma = 120^o$
Factor R			wRp = 3.72	Rp = 2.96	x^2 = 1.103

Table 3. Parameter structure, factor R and x^2 of $BaAl_xFe_{12-x}O_{19}$ (x = 2)

			Lattice Parameters		
Space Group	:	P 63/m m c			
Crystal system	:	Hexagonal	a = 5.88303 Å	b = 5.88303 Å	c = 23.17027 Å
Volume	:	694.448 Å^3			
Density (ρ)	:	5.016 g.cm^{-3}	$\alpha = 90^o$	$\beta = 90^o$	$\gamma = 120^o$
Factor R			wRp = 4.00	Rp = 3.15	x^2 = 1.133

Table 4. Parameter structure, factor R and x^2 of $BaAl_xFe_{12-x}O_{19}$ (x = 3)

			Lattice Parameters		
Space Group	:	P 63/m m c			
Crystal system	:	Hexagonal	a = 5.882072 Å	b = 5.882072 Å	c = 23.16498 Å
Volume	:	694.102 Å^3			
Density (ρ)	:	4.898 g.cm^{-3}	$\alpha = 90^o$	$\beta = 90^o$	$\gamma = 120^o$
Factor R			wRp = 4.00	Rp = 3.21	x^2 = 1.154

Table 5. Parameter structure, factor R and x^2 of $BaAl_xFe_{12-x}O_{19}$ (x = 4)

			Lattice Parameters		
Space Group	:	P 63/m m c			
Crystal system	:	Hexagonal	a = 5.88111 Å	b = 5.88111 Å	c = 23.16509 Å
Volume	:	693.879 Å^3			
Density (ρ)	:	4.787 g.cm^{-3}	$\alpha = 90^o$	$\beta = 90^o$	$\gamma = 120^o$
Factor R			wRp = 4.12	Rp = 3.27	x^2 = 1.119

Table 6. Parameter structure, factor R and x^2 of $BaAl_xFe_{12-x}O_{19}$ (x = 5)

Space Group : P 63/m m c		Lattice Parameters		
Crystal system : Hexagonal		a = 5.87847 Å	b = 5.87847 Å	c = 23.15467 Å
Volume : 692.945 Å^3				
Density (ρ) : 4.745 g.cm^{-3}		$\alpha = 90^o$	$\beta = 90^o$	$\gamma = 120^o$
Factor R		*wRp* = 4.25	Rp = 3.39	x^2 = 1.177

As for the case of x = 1 to 4 (see Table 2 – Table 6), no significant changes occurred. It indicated that after the addition of Al^{3+} ion does not form another phase and overall well-substituted with barium hexaferrite into the system. The lattice parameters decreased compared with the sample x = 0. The larger the value of x, the greater the decline in the value of the lattice parameter, and the value of Al^{3+} ion population factor (Factor R) was also gradually increasing. Many ion Al^{3+} substituted for Fe^{3+} in position 2a, followed on 12k, 2b, 4f1, and 4f2. While the sample x = 5, very different results than x = 0 - 4 is obtained, and also other phases of $BaAl_{2.18}Fe_{9.82}O_{19}$, namely Al_2O_3 and BaO were gained. Also, the sample x = 5 is also not a single phase. The lattice parameter in the sample x = 5 does not decline significantly as x = 0 - 4, the increase of the value of Al^{3+} ion population factor is not significant anymore, but it is not much different from the sample x = 4.

3.2. Raman Spectra

All peaks in the spectra are single phases of $BaFe_{12}O_{19}$, with no presence of any additional phase or an impurity. Since the laser power is limited, 10mW, no transformation of the compound into other phases or degradation was observed.

The peaks at 713 and 684 cm^{-1} can be assigned to A_{1g} vibrations of Fe-O bonds at the tetrahedral 4f1 and bipyramidal 2b sites, respectively. Other peaks at 614, 512, 467, 453 and 317 cm^{-1} are due to A_{1g} vibrations of Fe-O bonds at the octahedral 4f2, 2a, and 12k sites, whereas peak at 409 cm-1 is due to A_{1g} vibration at the octahedral 12k dominated site.

The peaks at 527, 285 and 212 cm^{-1} were due to E_{1g} vibrations, while the peak at 335 cm^{-1} was due to E_{2g} vibration. The peak at 184 and 173 cm^{-1} resulted from E_{1g} vibrations of the whole spinel block. The assignment of Raman spectra to the corresponding lattice symmetries are summarized in Table of Figure 4.

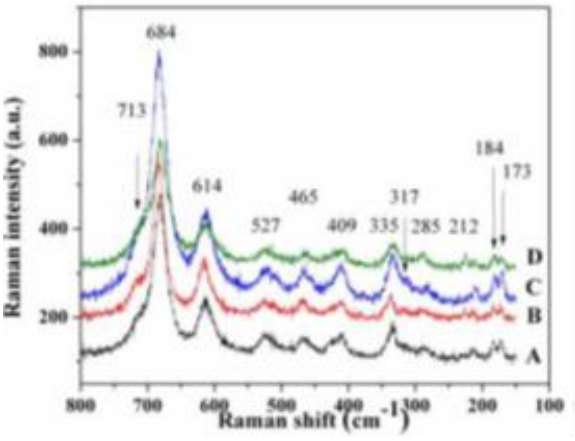

Raman active modes	Observed frequency (± 3 cm^{-1})	Assigned polyhedra
A_{1g}	713	Tetrahedra (*4f$_1$*)
	684	Bipyramid (*2b*)
	614	Octahedra (*4f$_2$*)
	512, 467, 453	Octahedra (*2a + 12k*)
	409	Octahedra (*12k*) dominated
	317	Octahedra *2a*
E_{1g}	527, 285, 212	---
	184, 173	Whole spinel block
E_{2g}	335	Octahedra *12k*

Figure 4. Raman spectra for Barium Hexaferrite $BaFe_{12-x}Al_xO_{19}$ with Al^{3+} ion substitution.

4. Conclusion

Substitution of Al^{3+} ion by Barium Hexaferrite gave an impact on the changes in crystal structure. The factor of Fe^{3+} ion population is slowly taken over by Al^{3+} ion in each position. The distances between the atoms became increasingly closer. Lattice parameter values decreased, resulting in decreasing the volume of the unit cell and atomic density. The ability of Al^{3+} ion substitution by an Fe^{3+} ion in this

Barium Hexaferrite system only up to the limit x until 4, which form the structure of $BaFe_8Al_4O_{19}$. The addition of Al^{3+} ion for x > 4 into the system of Barium Hexaferrite will form three phases, $BaFe_8Al_4O_{19}$, BaO and Al_2O_3, and the weight percent of BaO and Al_2O_3 phase will continue to increase. From the result of Raman Spectrum, the substitution of Al in the $BaFe_{12}O_{19}$ system leads to an increase in the intensity of resonance band when compared with the parent compound that indicates a significant variation of polarizability during the vibrations in the aluminum-substituted $BaFe_{12-x}Al_xO_{19}$ compounds.

5. References

[1] Pullar R C 2012 Hexagonal ferrites: A review of the synthesis, properties and applications of hexaferrite ceramics *Progress in Material Science* **57** 1191-1334.
[2] Arkel A E V *et al* 1936 *Rev. Trv. Chim.* **55** 331.
[3] Smit J *et al* 1959 Ferrites *Philips Technical Library* Eindhoven
[4] Nowosielski *et al* 2007 Barium ferrite powders prepared by milling and annealing *Journal of Achievements in Materials and Manufacturing Engineering* **28 (12)** 735-742.
[5] Obradors X *et al* 1985 X-ray analysis of the structural and dynamic properties of $BaFe_{12}O_{19}$ hexagonal ferrite at room temperature *Journal of Solid State Chemistry* **56** 171-181.
[6] Matsumoto M and Miyata Y 1996 A Gigahertz-range electromagnetic wave absorber with bandwidth made of hexagonal ferrite *J. Appl. Phys.* **79 (8)** 5486-5488.
[7] Adi W A and Manaf A 2012. Structural and absorption characteristics of Mn-Ti substituted Ba-Sr hexaferrite synthesized by mechanical alloying route *J. Basic. Appl. Sci. Res.* **2 (8)** 7826-7834.
[8] Sandiumenge F *et al* 1988. X-ray profile analysis of cation distribution in $SrAl_xFe_{12-x}O_{19}$ solid solution *Materials Research Bulletin* **23** 685-692.
[9] Shirtcliffe N J *et al* 2007 *Mater Res Bull* **42** 281.
[10] Umit Ozgur et al 2009 Microwave ferrites, part 1: fundamental properties J Mater. Sci: Mater. Electron. **20** 789 – 834
[11] Matsumoto M, Miyata Y 1996 A Gigahertz-range Electromagnetic Wave Absorber with Bandwidth Made of Hexagonal Ferrite. J. Appl. Phys., 79 (8): 5486-5488.
[12] Priyono and Azwar Manaf 2010 Magnetic material of M-type barium hexaferrite for material anti radar in the range of s-band frequency *Indonesian Journal of Materials Science* **11** 75 – 78.
[13] D Mishra *et al* 2003 X-ray diffraction studies on aluminium-substituted barium hexaferrite *Materials Letters* **58** 1147 – 1153.
[14] Vinod N *et al* 2011 Structural and magnetic behaviour of aluminium doped barium hexaferrite nanoparticles synthesized by solution combustion technique *Physica B* **406** 789 – 792.
[15] E J Mittemeijer and U Welzel 2013 Modern diffraction methods. *Wiley-VCH Germany* **xxvi** 519.
[16] Allen C Larson and Robert B Von Dreele 2004 GSAS : General structure analysis system *Los Alamos National Laboratory Report LAUR. California* 231.
[17] Wang X L *et al* 1994 Neutron diffraction measurements of the residual stresses in Al_2O_3 - ZrO_2 (CeO) ceramic composites *Journal of the American Ceramic Society* **77 (6)** 1569-1575.
[18] Wyckoff R W G 1963 Rocksalt structure. Crystal Structures *Second edition. Interscience Publishers, New York* **1** 85-237.

Acknowledgments
This work is supported in part by the DIPA of BATAN from Ministry of Finance Year 2015.